

Modelling and Design of Optimal Internal Loop Air-Lift Reactor Configurations Through Computational Fluid Dynamics

Fernando Ramonet*, Bahram Haddadi, Christian Jordan, Michael Harasek

Technische Universität Wien, Institute of Chemical Environmental and Bioscience Engineering, Getreidemarkt 9/166, 1060 Wien, Austria.

fernando.ramonet@tuwien.ac.at

With the current shift from a fossil-based to a biomass-based economy, the study of biorefineries and their main components has gained significant importance. The main components of biorefineries include bioreactors. For many systems, the improvement of mass transfer in and between phases through mixing is the key success factor. So far, many studies have focused on mechanically stirred reactors, but not many on pneumatically stirred systems.

Air-lift reactors (ALR) are widely used in the chemical, biochemical and pharmaceutical industries. ALR inserts allow better flow control. Critical design parameters for ALR with such circular-loops are liquid and gas recirculation. The proper design and placement of these inserts, so-called draft tubes, is essential and has a significant influence on two-phase hydrodynamics as well as on mass transfer in the reactor since the draft tube guides the flow field. In this study, we use computational fluid dynamics (CFD) to characterize the flow of three different internal loop ALR geometries with different internal configurations (single and double draft tubes). Design parameter variations of the studied ALRs will allow the prediction of optimal configurations for bioreactors, e.g. in more efficient biorefinery concepts. No previous CFD studies have been found in literature comparing the flow of single stage and multi-stage internal loop ALRs. Higher mixing intensities were achieved in the upper part of the double stage internal loop ALR, the ratio between the bioreactor and the draft tube has an effect on the downcomer velocity.

1. Introduction

Biomass is transformed into biomaterials, biochemicals and bioenergy in biorefineries. One of the main components of biorefineries are bioreactors. State-of-the-art bioreactors are needed to produce high-quality biochemicals and biomaterials. A special interest is put in the Air Lift Reactor (ALR), with both its variations internal loop and external loop, due to its low shear forces while mixing.

The ALR consists of a riser and a downcomer, a pressure gradient formed by the mean density between the riser and the downcomer is utilized as a pneumatic mixing strategy. The main applications, characteristics, and design considerations of ALRs were reviewed by Chisti and Young (1987). Several studies in ALRs have addressed liquid mixing, fluid velocities, and gas hold-up. Verlaan et al. (1989) developed a model to predict liquid velocities and local gas hold-ups in external loop ALRs. Lu et al. (1994) experimentally studied liquid mixing in two and three-phase internal loop airlift reactors. Blenke (1979) performed one of the first studies in loop reactors. According to Blenke (1979), a substantial shortening in mixing time can be achieved when dividing the draft tube into 2 or 3 sections.

The first appearances of multi-stage concentric draft tube geometries were in the works of Blenke (1979) as divided draft tubes for shortening mixing time up to 80 % for double draft tube and up to 87.50 % in triple draft tube, and Petersen and Margaritis (2001) as staged internal loop gas lift bioreactor.

Due to the increasing need for more efficient reactors, in recent years multi-stage internal loop ALRs have become a topic of interest in research. Li and Qi (2014) studied the hydrodynamics and flow regimes of a multi-stage internal loop ALR. Li et al. (2018) studied the hydrodynamics and bubble behaviour in a three-phase two-

stage internal loop ALR. Tao et al. (2020) performed an experimental investigation of the hydrodynamics (flow regime, liquid circulating velocity, gas hold-up, and mixing time) and the mass transfer in a three-stage internal loop ALR to reveal the difference between the gas-liquid bubbly flow and the gas-liquid-solid slurry flow. Zhang et al. (2012) utilized computational fluid dynamics (CFD) to predict the hydrodynamics of an enhanced ALR. Shi et al. (2021) studied a two-stage internal loop ALR with contraction-expansion vane with CFD. Air lift reactors with internal loop utilized as gas lift or air lift bioreactors are a promising technology for biological processes due to their low shear stress, great heat and mass transfer properties.

2. Materials and methods

Computational simulations are a tool to represent real-world systems and processes by means of mathematical models. Simulations can decrease the costs of experiments in a precise and reproducible manner. Horvath et al. (2009) performed an analysis of the difference between an experiment on an internal loop split ALR and simulations in commercial and open-source software.

In this study, CFD is utilized to characterize the flow of three different internal loop ALR geometries with different internal configurations (single and double draft tubes).

2.1. Development of CFD Model

The software Open-source Field Operation And Manipulation (OpenFOAM) version 9 with the standard *multiphaseEulerFoam* solver was used to resolve the hydrodynamic CFD calculations for every geometry. The standard *multiphaseEulerFoam* solver is ideal for modelling gas bubbles in a liquid since it solves two or more compressible fluid phases with at least one dispersed phase. Air was used for the dispersed phase and water for the continuous. OpenFOAM utilizes the finite volume method to resolve the equations, and the pressure-velocity coupling is solved with the PIMPLE algorithm (Passalacqua and Fox, 2011).

For solving the air turbulence, the *ContinuosgaskEqn* large-eddy simulations sub-grid model was utilized to resolve the gas phase. The *ContinuosgaskEqn* consists of a one-equation sub-grid stress model for the gas (dispersed) phase in a two-phase system that supports phase-inversion (OpenCFD Ltd., 2019).

For solving the water turbulence, the *NicenoKEqn* large-eddy simulations sub-grid model was utilized to resolve the fluid phase. The *NicenoKEqn* is a one-equation sub-grid stress model for the continuous phase in a two-phase system including bubble-generated turbulence (Ničeno et al., 2008).

For the properties of the phases, the *SchillerNeumanModel* (Schiller, 1933) was utilized for the drag of each phase. The diameter of the bubbles was set to 4.5 mm, according to van Baten et al. (2003), the rise velocity is practically independent of the bubble size in the 3 to 8 mm range. Values found in the literature go from 3 mm to 5 mm. The diameter of the water particles is set to 0.1 mm.

The typical operating superficial gas velocity range for bioprocesses is between 7.6×10^{-4} m/s and 0.05 m/s (Luo and Al-Dahhan, 2011). For low gas input rates up to 0.04 m/s, the liquid velocities in the riser (upcomer) and downcomer are very sensitive to changes in gas input rate (Gavrilescu and Tudose, 1995). For this study three different velocities were chosen, 0.01, 0.02, and 0.04 m/s.

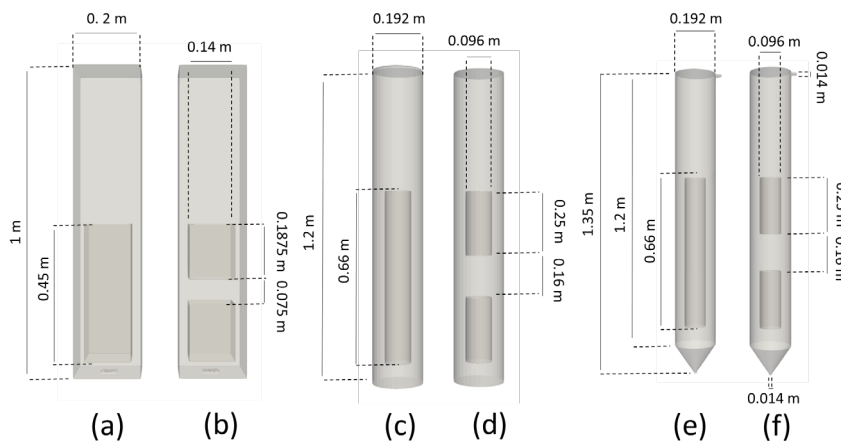


Figure 1: Air-lift reactors (a) Squared Single Draft (SSD) tube geometry from Jia et al. (2007), (b) Squared Double Draft (SDD) tube geometry, (c) Cylindrical Single Draft (CSD) tube geometry, (d) Cylindrical Double Draft (CDD) tube geometry from Shi et al. (2021), (e) coned bottom cylindrical Single Draft tube Geometry (SDG), (f) coned bottom cylindrical Double Draft tube Geometry (DDG).

Three ALR representing geometries were evaluated in this study. A squared geometry from Jia et al. (2007), a cylindrical geometry from Shi et al. (2021), and a coned bottom cylindrical geometry. The squared reactor geometry from Jia et al. (2007) consists of a rectangular vessel of 1 m x 0.2 m x 0.2 m. The draft tube is 0.45 m x 0.14 m x 0.14 m and the inlet consists of 169 holes of 1 mm in diameter. Two gas inlet velocities were chosen from the paper, 0.1 m/s and 0.2 m/s, to evaluate how the velocity affects the reactor's mixing performance. Liquid height was set to 0.6 m. The distance from the inlet to the bottom of the draft tube section is 0.04 m. The cylindrical double draft tube geometry from Shi et al. (2021) consists of a cylindrical vessel with a radius of 0.1 m x 1.2 m in height, two draft tubes with a radius of 0.05 m and 0.25 m in height, separated from each other by 0.16 m, a distance from the inlet to the bottom of the first draft tube of 0.08 m. The gas inlet consists of 13 holes with a diameter of 0.5 mm. Liquid height at 1 m and the distance from the inlet to the bottom of the draft tube section is 0.0075 m.

The third geometry consists of a cylindrical reactor similar to the second geometry, with the coned transition from the inlet to the body. The liquid level is set to 1 m and the distance from the inlet to the bottom of the draft tube section is 0.1875 m. Figure 1, shows the dimensions of the three chosen geometries with single and double draft tubes.

The boundary conditions were reproduced from the literature. For the squared geometry (Figures 1a and 1b) from Jia et al. (2007) and for the cylindrical geometry (Figures 1c and 1d) from Shi et al. (2021). For the coned bottom cylindrical geometry (Figures 1e and 1f), the boundary conditions of Shi et al. (2021) were also used.

The six geometries were meshed with the OpenFOAM mesh generation tool *snappyHexMesh*. Table 1 shows the cell count, maximum skewness, and maximum non-orthogonality of the meshes. The mesh quality recommended in OpenFOAM is a maximum non-orthogonality of 70° and a maximum skewness of around 4 (Greenshields, 2021).

A grid independency study was performed with the coned bottom bioreactor without a draft tube to find an optimal mesh. Air velocity values were extracted in diagonal from inlet to outlet. A total of five meshes were utilized with a refinement factor of 1.5, ranging from 23 thousand to 2.2 million cells. The first three meshes were utilized to determine the order of convergence. The Richardson extrapolation (Richards, 1997) was used to verify the convergence between the calculated values (extrapolated) and extracted values of meshes 4 and 5, with an error of 0.38 % and 0.74 %.

Table 1: Mesh properties.

Properties	SSD	SDD	CSD	CDD	SDG	DDG
Cells	672,172	681,806	320,430	641,705	445,808	645,772
Maximum Skewness	4.21	4.41	3.2	4.48	4.71	3.26
Maximum Non-orthogonality	53.96	52.50	63.56	64.80	55.29	53.51

3. Results

A total of 9 cases were simulated with the three geometries. The Squared Single Draft (SSD) tube geometry from Jia et al. (2007) and the Squared Double Draft (SDD) tube geometry were simulated with 0.01 m/s and 0.02 m/s. The Cylindrical Double Draft (CDD) tube geometry from Shi et al. (2021) was simulated with 0.01 m/s and 0.04 m/s. The Cylindrical Single Draft (CSD) tube geometry, the coned bottom cylindrical Single Draft Tube Geometry (SDG) and the coned bottom cylindrical Double Draft tube Geometry (DDG) were simulated with 0.04 m/s. The simulation time for each case to reach 60 seconds of computation time is shown in Table 2 with the utilized cores. In the cases shown in Table 2, the first three letters represent which geometry, and the two digits represent the decimal points of the velocities in m/s. Cases SDD02 and CSD04 are still in computation at the time of this publication. The flow from the three geometries is compared in Figure 2(a), (b) and (c) with a single and double draft tube. Figure 2(b) compares the flow at 26.1 seconds since the simulation from case CSD04 is still running. In Figure 2 (a) and (d) it can be seen the developed axial velocities from the upcomer and downcomer. In Figure 2(b), it can be seen at the current state of the simulation that there is no developed flow in the bottom draft tube as it can be seen from Figure 2(a) and Figure 2(c). Figure 2(a), (b) and (c) show the different fluid heights inside the reactors, which are related to the development of the downcomer velocity. Maximum downcomer velocity of 0.15 m/s was reported in Figure 2 for the squared geometry and 0.03 m/s for the cylindrical geometries. In Table 3, different parameters from the simulated geometries are presented. For the single draft tube geometries, the draft tube loop circulation time is presented under the column "first". For the double draft tube geometries, the loop circulation time for the draft tube on top is presented under the column

“first”. The loop circulation time on the bottom draft tube on the double draft tube geometries is presented under the column “second”. The yellow line in Figure 2(d) represents the first loop in the double draft tube geometries, while the green line represents the second loop.

Table 2: Summary from computation.

Case	Simulation Time (s)	Computation Time (h)	Cores	Timestep (s)
SSD01	60	650	4	5×10^{-4}
SSD02	60	797	4	5×10^{-4}
SDD01	60	656	4	5×10^{-4}
SDD02	34.64	1709	8	1×10^{-4} *
CSD04	34.27	1651	4	1×10^{-4} *
CDD01	60	198	4	1×10^{-3}
CDD04	60	207	4	1×10^{-3}
SDG04	60	59	4	1×10^{-3} *
DDG04	60	81	4	1×10^{-4} *

* Adjustable timestep, self-calculated by the algorithm depending on the timestep's Courant number.

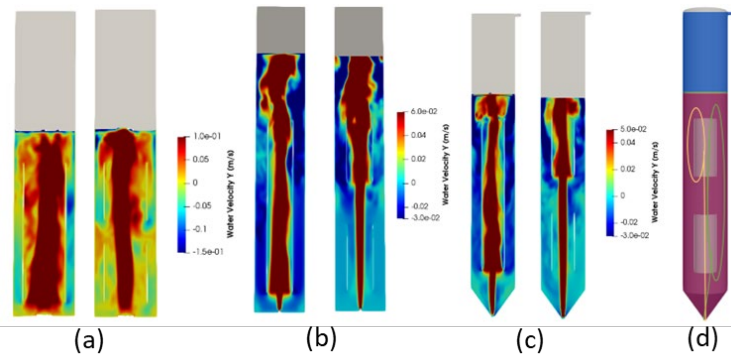


Figure 2: (a) Water velocity comparison on the Y-axis of cases SSD01 and SDD01 at 60 s, (b) water velocity comparison on the Y-axis of cases CSD04 and CDD04 at 26.1 s, (c) water velocity comparison on the Y-axis of cases SDG04 and DDG04 at 60 s, (d) loop circulation for double draft tube geometries.

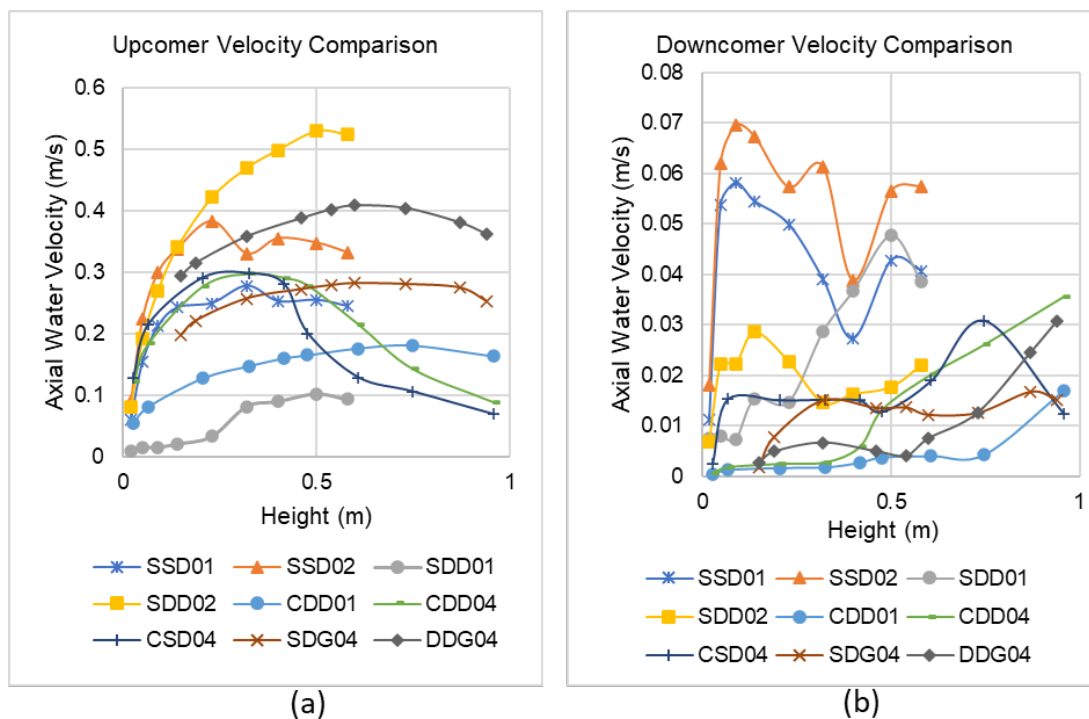
For Table 3, two points on the downcomer side were sampled, one at the bottom of the reactor between the bottom and the draft tube and a second at the top, between the draft tube and the fluid's level. The turbulence kinetic energy of the fluid phase, the fluid's velocity, and the pressure for the two sampled points are shown in Table 3.

Even though for geometries SSD and SDD, lower velocities were used for the inlet, higher downcomer velocities can be observed at the bottom measured point, which is caused by the pressure increase due to the ratio from reactor diameter versus draft tube diameter. Geometries CSD and CDD have lower turbulent kinetic energy in both top and bottom points due to the distance between the top of the draft tube and the liquid's surface area. Regarding the draft tube loop circulation time, the worst performing is CDD04.

Table 3: Obtained results.

Case	Turbulence kinetic energy in fluid phase (m^2/s^2)		Fluid velocity on Y-axis (m/s)		Pressure (mbar)		Draft tube loop circulation time (s)	
	Top	Bottom	Top	Bottom	Top	Bottom	First	Second
SSD01	5.87×10^{-4}	1.36×10^{-4}	0.028	0.02	1,127	1,182	16.56	-
SSD02	2.02×10^{-4}	8.24×10^{-5}	0.04	0.07	1,269	1,321	12.28	-
SDD01	6.73×10^{-4}	2.82×10^{-5}	0.018	0.02	1,125	1,180	34.85	54.22
SDD02	3.22×10^{-4}	2.29×10^{-6}	0.04	0.006	1,045	1,097	24.76	32.37
CSD04	6.18×10^{-5}	1.95×10^{-6}	0.035	0.019	1,004	1,074	145.36	-
CDD01	1.44×10^{-4}	1.36×10^{-6}	0.007	0.001	1,004	1,095	27.52	45.04
CDD04	2.21×10^{-4}	7.52×10^{-7}	0.043	0.001	1,004	1,077	20.70	146.06
SDG04	4.48×10^{-5}	2.14×10^{-6}	0.018	0.006	1,004	1,077	53.40	-
DDG04	1.28×10^{-4}	1.04×10^{-6}	0.033	0.007	1,004	1,077	26.91	110.76

Figure 3(a) and Figure 3(b) show the upcomer velocity and downcomer axial water velocity respectively. The upcomer velocity was measured inline from the center of the draft tube(s), while the downcomer velocity was measured inline centered from the space between the draft tube(s) and the vessel. The presented results were time-averaged from 0.5 – 60 s for quantitative comparison. For cases SDD02 and CSD04 the results were time averaged from 0.5 s to the reported time in Table 2. The Figures show absolute values of the axial velocities. Joshi et al. (1990) reported that for air lift reactors with internal loop the optimal values of height to diameter ratio, area ratio and reactor volume are different for different design case depending on the objectives such as overall liquid circulation rate, mass transfer rate effective interfacial area, and extent of mixing. When adding a second draft tube, it has been found that the mixing in the reactor is enhanced. On the double draft tube geometries, lower circulation rates were found on the bottom draft tube. According to Figure 3(a), geometry SDD performs poorly with low inlet velocity values compared to geometry SSD. When the inlet velocity is increased for 0.01 to 0.02 m/s, the SDD geometry reaches higher upcomer velocity than the other five configurations. The highest upcomer velocities were found in case SDD02. From Figure 3(b), it can be seen, that higher downcomer velocities are achieved on the squared bioreactor geometries due to the pressure difference created by the vessel-draft tube ratio and the distance between the interphase surface and the end of the draft tube area.



Geometries comparison of water (a) upcomer and (b) downcomer velocity.

Figure 3(b) shows that higher downcomer velocities are achieved on the single draft tube geometries. A detailed study comparing the downcomer velocities with the turbulent kinetic energy is needed to determine how dividing the draft tube in to two or more sections affects the overall mixing. Further research is needed to evaluate if the distance between draft tubes and the ratio of draft tube diameter versus reactor diameter affects the flow inside the reactor.

4. Conclusions

In this study, different internal reactor configurations were compared for air lift reactors with computational fluid dynamics. Out of the three compared geometries the squared single and double draft tube reactor had a higher downcomer velocity, higher turbulence kinetic energy and lower loop circulation time. When comparing single and double draft tube internal configurations, it was found that the flow reaches a higher turbulent kinetic energy in the upper part of the double draft tube configurations. The ratio of the draft tube-vessel width and the distance

between the draft tube and the fluid's surface has proven to have an effect on the draft tube's loop circulation time. The internal geometry of air-lift reactors has proven to influence the downcomer velocity. Further research is needed to determine the flow's behavior when utilizing different draft tube parameters such as distance from the draft tube to the surface, the distance between draft tubes, length of draft tubes, and diameter of draft tubes.

Acknowledgments

This project has received funding from the European Union's Horizon 2020 research and innovation programme under the Marie Skłodowska-Curie grant agreement N° 860477, 'AgRefine'.

References

- Blenke H., 1979, Loop reactors. *Advances in Biochemical Engineering*, 13, 121–214.
- Chisti M. Y., Moo-Young M., 1987, Airlift reactors: characteristics, applications, and design considerations. *Chemical Engineering Communications*, 60(1-6), 195-242.
- Gavrilescu M. and Tudose R.Z., 1995. Study of the liquid circulation velocity in external-loop airlift bioreactors. *Bioprocess Engineering*, 14(1), 33–39.
- Greenshields C., 2021, OpenFOAM User Guide. OpenFOAM Foundation Ltd. Available at: <openfoam.org> accessed 20.04.2022.
- Horvath A., Jordan C., Lukasser M., Kuttner C., Makaruk A., Harasek M., 2009. CFD Simulation of bubble columns using the VOF Model - Comparison of commercial and open source solvers with an experiment. *Chemical Engineering Transactions*, 18, 605–610.
- Jia X., Wen, J., Feng W., Yuan Q., 2007, Local hydrodynamics modeling of a gas– liquid– solid three-phase airlift loop reactor. *Industrial & engineering chemistry research*, 46(15), 5210-5220.
- Joshi J.B., Ranade V. v., Gharat S.D., Lele S.S., 1990, Sparged loop reactors. *The Canadian Journal of Chemical Engineering*, 68(5), 705–741.
- Li D., Guo K., Li J., Huang Y., Zhou J., Liu H., Liu C., 2018, Hydrodynamics and bubble behaviour in a three-phase two-stage internal loop airlift reactor. *Chinese Journal of Chemical Engineering*, 26(6), 1359–1369.
- Li S., Qi T., 2014. Hydrodynamics and flow regimes of a multi-stage internal airlift loop reactor. *Materials Focus*, 3(3), 205–210.
- Lu W. J., Hwang S. J., Chang C. M., 1994, Liquid mixing in internal loop airlift reactors. *Industrial & Engineering Chemistry Research*, 33(9), 2180-2186.
- Luo H.P., Al-Dahhan M.H., 2011, Verification and validation of CFD simulations for local flow dynamics in a draft tube airlift bioreactor. *Chemical Engineering Science*, 66(5), 907–923.
- Ničeno B., Dhotre M.T., Deen N.G., 2008, One-equation sub-grid scale (SGS) modelling for Euler–Euler large eddy simulation (EELES) of dispersed bubbly flow, *Chemical Engineering Science*, 63(15), 3923–3931.
- OpenCFD Ltd., 2019. OpenFOAM Guide. <www.openfoam.com/documentation/guides/latest/api/classFoam_1_1LESModels_1_1continuousGasKEqn.html> accessed 20.04.2022.
- Passalacqua A., Fox R.O., 2011, Implementation of an iterative solution procedure for multi-fluid gas–particle flow models on unstructured grids. *Powder Technology*, 213(1–3), pp.174–187.
- Petersen E. E., Margaritis A., 2001, Hydrodynamic and mass transfer characteristics of three-phase gaslift bioreactor systems. *Critical Reviews in Biotechnology*, 21(4), 233-294.
- Richards S. A., 1997, Completed Richardson extrapolation in space and time. *Communications in Numerical Methods in Engineering*, 13(7), 573-582.
- Schiller L., 1933, A drag coefficient correlation. *Zeit. Ver. Deutsch.*, 77, 318–320.
- Shi J., Guo K., Wang Z., Zheng L., Liu H., Xiang W., Liu C., Li X., 2021, Computational Fluid Dynamics Simulation of hydrodynamics in a two-stage internal loop airlift reactor with contraction-expansion guide vane. *ACS Omega*, 6(10), 6981–6995.
- Tao J., Huang J., Geng S., Gao F., He T., Huang Q., 2020, Experimental investigation of hydrodynamics and mass transfer in a slurry multistage internal airlift loop reactor. *Chemical Engineering Journal*, 386, 122769.
- van Baten J.M., Ellenberger J., Krishna R., 2003, Hydrodynamics of internal air-lift reactors: experiments versus CFD simulations. *Chemical Engineering and Processing: Process Intensification*, 42(10), 733–742.
- Verlaan P., van Eijs A.M.M., Tramper J., Riet K.V. t., Luyben K.C.A.M., 1989, Estimation of axial dispersion in individual sections of an airlift-loop reactor. *Chemical Engineering Science*, 44(5), 1139–1146.
- Zhang T., Wei C., Feng C., Zhu J., 2012, A novel airlift reactor enhanced by funnel internals and hydrodynamics prediction by the CFD method. *Bioresource Technology*, 104, 600–607.